

Stress evolution during ultrasonic Al ribbon bonding

Masaya Ando¹, Kazumasa Takashima¹, Masakatsu Maeda²
and Yasuo Takahashi²

¹ Graduate School of Engineering, Osaka University, 2-1 Yamadaoka, Suita, Osaka 565-0871, Japan

² Joining and Welding Research Institute, Osaka University, 11-1 Mihogaoka, Ibaraki, Osaka 567-0047, Japan

E-mail: takasy@jwri.osaka-u.ac.jp

Abstract. The present study reveals the stress distribution in the substrate during ultrasonic bonding. The deformations of the Si substrate, Al ribbon, and Al pad were numerically analyzed using a finite element method. Experimental observation of the interface using a high-speed video camera was also conducted to determine the actual interfacial slip amplitude. This amplitude becomes smaller than that of tool-tip with bonding time. It was suggested from the numerical simulations that frictional adhesion enhanced the friction force, resulting in an increase in the equivalent stress in the ribbon and pad. As a result, very large stresses occur in the substrate during ultrasonic bonding. These stresses evolve with the progress of ultrasonic bonding, i.e., frictional adhesion.

1. Introduction

Ultrasonic bonding of thick Al ribbon is necessary for packaging heavy-duty power electronics devices. However, the under-pad structures of the power electronics devices can be damaged by the large interfacial shear stresses that emerge during ultrasonic bonding [1]. To overcome this problem, it is important to understand and control stress evolution during the bonding process. The stress distribution in an Al ribbon and a pad electrode has been investigated by numerical simulation [2, 3], and this simulation has to be extended to the under-pad structure to understand its influence on failure behavior. The present study reports on the stress distribution in the substrate during ultrasonic bonding.

Many *in-situ* measurements and observations have been made in order to understand the phenomena present during ultrasonic bonding [4-6]. Vibration amplitude at the tool-tip is one of the important parameters related to the state of bonding [7-9]. However, there are no reports about actual interfacial slide. It is supposed that the vibration amplitude is different between the tool-tip and the interface. It is important to understand the origin of this amplitude difference because it is a significant parameter in numerical simulations. Another purpose of the present study is to determine the actual vibration amplitude at the bonding interface during ultrasonic bonding.

2. Experimental procedure

The interface between SiO₂ substrate and Al ribbon during bonding was observed with a high-speed video camera (HX-3, nac Image Technology, Japan). The ultrasonic bonding apparatus used in the present study is schematically illustrated in Figure 1. A transparent SiO₂ substrate was used to observe the interface from the underside of the device. The thickness and width of Al ribbon were 0.2 mm and



1.0 mm, respectively. The thickness of the SiO₂ substrate was 2.0 mm. The bonding tool was made of tungsten carbide. The vibration direction was parallel to the longitudinal direction of the Al ribbon. The ultrasonic frequency f was 60 kHz. The bonding force F_b was 7.0 N, which was comparable to the bonding pressure $P_b = 28$ MPa in the numerical simulation. The ultrasonic power P_u was 3.0 W. The ultrasonic vibration was applied for 400 ms. The frame rate of the video camera was 5×10^5 fps, which is sufficient for tracking the actual motion of the ribbon at the interface during ultrasonic bonding. The video data was analyzed to determine the amplitude at the interface by tracking the motion of a certain point in the interface during bonding. Simultaneously, the vibration amplitude at the tip of the wedge tool was monitored with a laser-Doppler vibrometer.

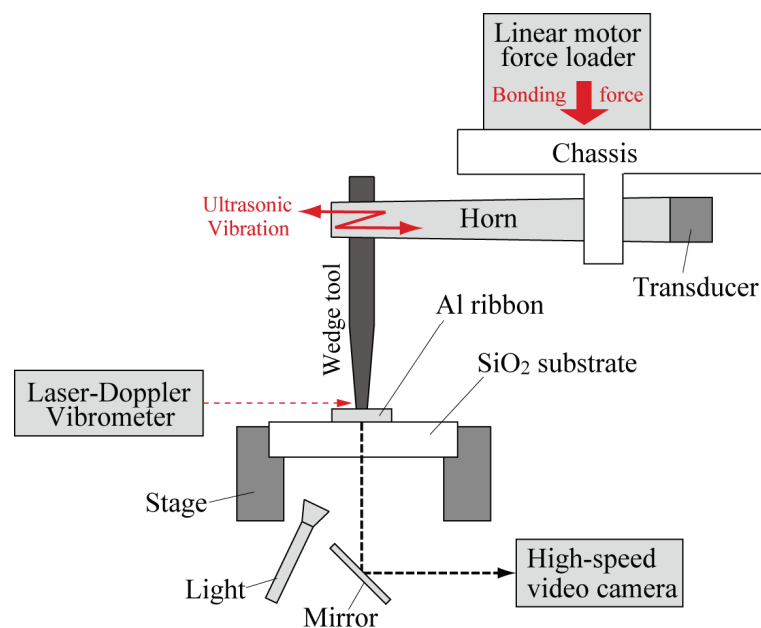


Figure 1. Schematic illustration of the ultrasonic bonding apparatus and measuring system.

3. Numerical procedure

The numerical analysis was performed using a finite element method. The mesh pattern used is illustrated in Figure 2. The thickness of Al ribbon was 200 μm . The thickness and width of the electric pad were 3–10 μm and 500 μm , respectively. The initial contact width was 250 μm . The ultrasonic frequency f was 60 kHz, equal to that in the experimental condition. The bonding pressure P_b was 28 MPa.

The temperatures of the ribbon and pad change with bonding time because of friction heating at the interface, and this temperature change should be considered. However, the numerical calculation will be a very hard task. So, the temperatures of the Al ribbon and the Al pad were assumed to be approximately constant at 373 K in the numerical simulations. This assumption is appropriate for estimating the stress evolution of the substrate during the ultrasonic bonding process and is based on the previous numerical and experimental study [2, 3]. Also, the substrate under the pad will be heated by friction. However, it was assumed that materials constants of the SiO₂ substrate were almost constant in the temperature range of 273–373 K. That is, the temperature of the SiO₂ substrate was fixed at 293 K, and we used the elastic constants of SiO₂ at 293 K for the substrate.

Because frictional slip occurs at the interface between the ribbon and pad, the deformations of the ribbon and pad were calculated separately as in a two-body problem [3]. It was assumed that the Al ribbon and Al pad were visco-plastic bodies and that the Si substrate was a perfectly elastic body. The visco-plastic deformation of the Al ribbon and Al pad were calculated according to the previous

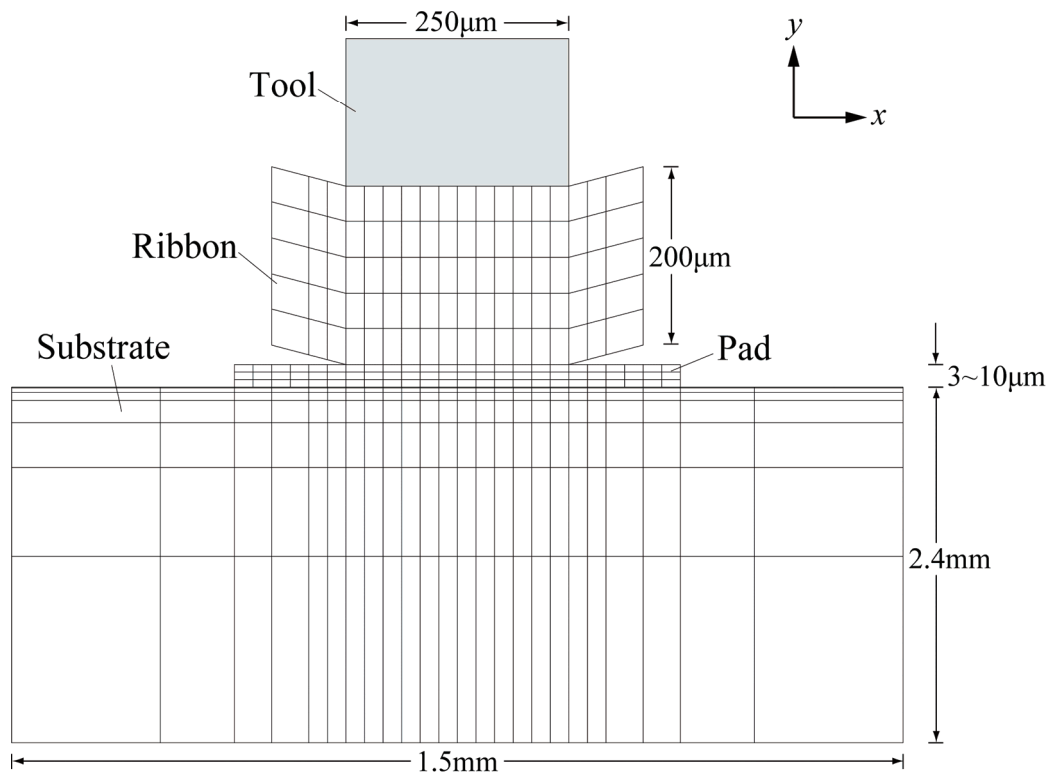


Figure 2. Mesh pattern in cross-section of the tool, Al ribbon, Al pad, and substrate.

studies [2, 3]. It was also assumed that the interface between the pad and SiO₂ substrate was fixed without any frictional slip.

The detailed procedure for this calculation is in [2, 3]. However, the size of this model is different from that of the previous study. In the present study, the model is enlarged to fit the experimental size. The vibration amplitude A_o and the amplitude at the bottom of the ribbon A_b was changed based on experimental results. These amplitudes are important parameters which show the state of the bonding interface. The decrease in A_b represents the fact that the constraint on the interface becomes stronger as adhesion progresses.

The elastic deformation of the substrate was calculated using CAE software (Sanseikai, Japan). It was assumed that the force was balanced between the bottom of the pad and the top of the substrate, i.e., the nodal force of pad-bottom was equal to that of substrate-top. The material constants of SiO₂ substrate were taken from the literature [10]. The change in stress in the substrate with time was simulated and compared with the experimental results. The shear stress applied at the interface between the Al ribbon and the SiO₂ substrate was measured using a piezoelectric load cell. The detailed monitoring procedure is described in [1]. Experimental condition was $F_b = 7.0$ N, $P_u = 2.5$ W, $f = 60$ kHz. The ultrasonic vibration was applied for 400 ms.

4. Results and discussion

Figure 3 shows the experimental results for the amplitudes of both the tool-tip A_t and bonding interface A_i over the range of bonding times t of 1–100 ms. The bonding condition was $F_b = 7.0$ N, $P_u = 3.0$ W. A_i could not be determined after $t = 100$ ms because the motion was too small to track given the resolution of the video camera. At $t = 1$ and 5 ms, A_i is slightly larger than A_t , but this may be because of the measuring accuracy of A_i . It is supposed that the ribbon slides on the substrate almost freely, i.e., $A_i \approx A_t$, at the beginning of bonding. After $t = 10$ ms, A_i begins to decrease with bonding time. On the other hand, A_t becomes smaller than A_i and the difference between A_i and A_t increases with progress of the bonding process. *In-situ* observations indicate that adhered areas at the interface expand with bonding time [11], and the Al ribbon becomes increasingly constrained.

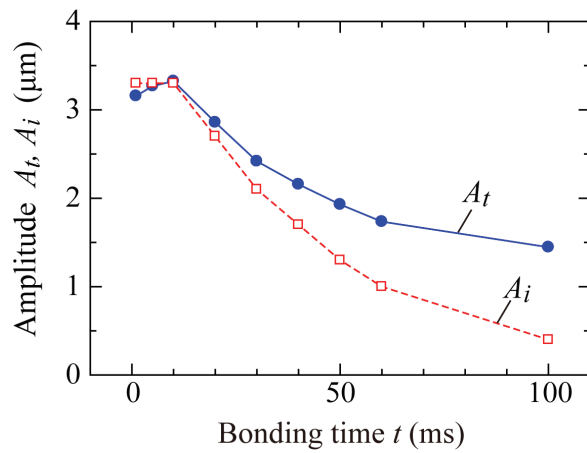


Figure 3. Experimental results for the amplitudes of the tool-tip and bonding interface vs. bonding time. The bonding condition was $F_b = 7.0$ N, $P_u = 3.0$ W.

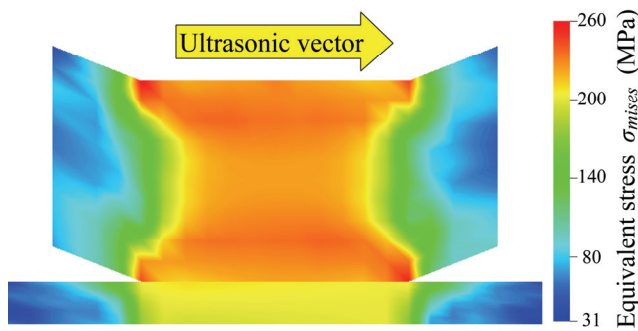


Figure 4. Equivalent stress distribution of the ribbon and pad. The parameters for the calculation are $A_o = 3.5$ μm , $A_b = 3.4965$ μm , $T = 373$ K, and $t_p = 4$ μm .

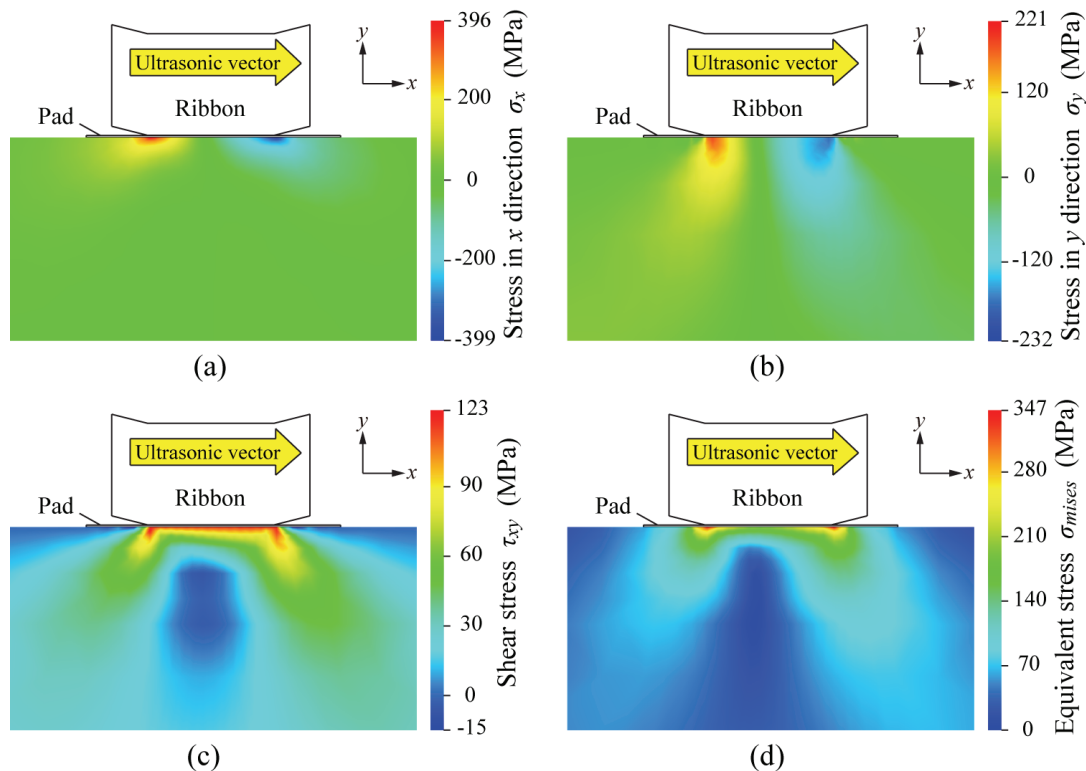


Figure 5. Distribution of (a) σ_x , (b) σ_y , (c) τ_{xy} , and (d) the equivalent stress σ_{mises} in the substrate. The calculations were performed using $A_o = 3.5$ μm , $A_b = 3.4965$ μm , $T = 298$ K and $t_p = 4$ μm .

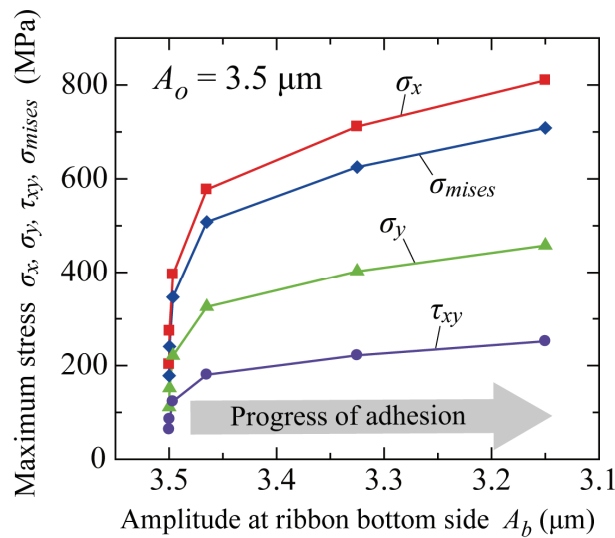


Figure 6. Change in the maximum stresses in substrate σ_x , σ_y , τ_{xy} , and equivalent stress σ_{mises} with the progression of adhesion. The decrease in A_b represents that the constraint of the interface increasing with the progress of adhesion.

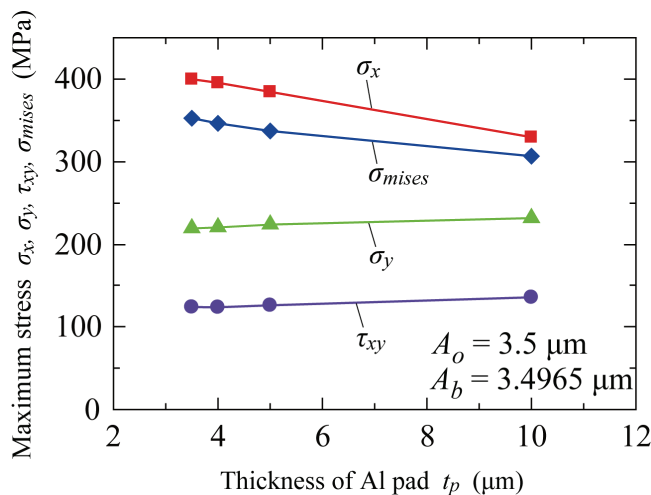


Figure 7. Change of the maximum stress in the substrate σ_x , σ_y , τ_{xy} , and the equivalent stress σ_{mises} depending on the thickness of Al pad.

Figure 4 shows the equivalent stress distribution of the ribbon and pad. The parameters for the calculation were $A_o = 3.5 \mu\text{m}$, $A_b = 3.4965 \mu\text{m}$, temperature $T = 373 \text{ K}$, and thickness of Al pad $t_p = 4 \mu\text{m}$. The thickness of the pad has been magnified 10 times for illustration purposes. This calculated distribution results when the ultrasonic vibration is applied from the left- to the right-hand side. A_b is 0.999 times as small as A_o . A large equivalent stress develops in the ribbon and pad even though A_b is just slightly smaller than A_o . Figure 5 shows the distribution of (a) the stress in x -direction σ_x , (b) the stress in y -direction σ_y , (c) the shear stress τ_{xy} , and (d) the equivalent stress σ_{mises} in substrate. The calculation parameters were the same as in Figure 4. The x -direction is in parallel to the vibration direction, and the y -direction is perpendicular to x -direction. In Figures 5(a) and (b), positive values indicate tensile stresses and negative value indicate compressive stresses. σ_x emerges just under the edge of the interface; it is tensile at the left-hand side and compressive at the right-hand side. This tensile and compressive σ_x is caused by shear stress in the interface. The distribution of σ_y is similar to that of σ_x but it spreads in the y -direction. Although the ultrasonic vibration is applied in the x -direction, a moment is applied to the ribbon [3]; this moment causes tensile and compressive σ_y . As seen in Figure 5(c), a large τ_{xy} develops under the interface. The interfacial shear stress during bonding produces this large τ_{xy} in the substrate. The maximum σ_{mises} is approximately 347 MPa, which is considerably larger than the bonding pressure.

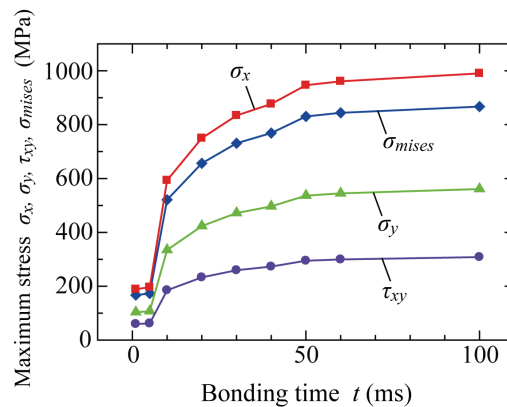


Figure 8. Change of maximum stresses in substrate σ_x , σ_y , τ_{xy} and equivalent stress σ_{mises} with bonding time.

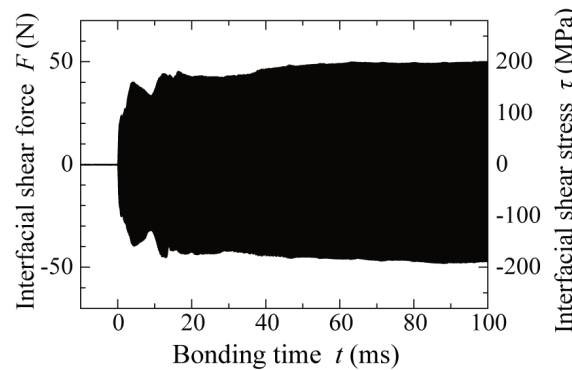


Figure 9. Experimental results of interfacial shear stress. The bonding condition was $F_b = 7.0$ N, $P_u = 2.5$ W.

As described in the numerical procedure, the decrease in A_b represents the enhancement of the constraint of interface with the progress of adhesion. Figure 6 shows the change of the maximum stresses in substrate with the progress of adhesion. The calculation parameters were $A_o/\mu\text{m} = 3.5$ and $3.5 > A_b/\mu\text{m} > 3.1$, $T = 373$ K, and $t_p = 4$ μm . That is, A_o was fixed and only A_b was altered in Figure 6 in order to investigate the influence of the difference between A_o and A_b on progress of adhesion. As frictional adhesion increases and the adhesion areas expand in the interface, large stresses develop in the interface [2], and the maximum stresses in the substrate also increase. As seen in Figure 6, the maximum stresses rapidly increase when A_b is just slightly smaller than A_o . This suggests that even though the adhered areas are very small in the bonding interface, stress is significantly enhanced in the substrate.

Figure 7 shows the change in the maximum stresses in substrate with the thickness of the Al pad. The calculation parameters were $t_p = 3, 4, 5, 10$ μm , $A_o = 3.5$ μm , $A_b = 3.4965$ μm , and $T = 373$ K. σ_x is reduced by increasing the thickness of the Al pad. It is suggested that stress in x -direction is buffered by a thick Al pad. In contrast, σ_y and τ_{xy} slightly increase with increasing t_p . This slight increase could be related to convergence error of the displacement rates within the pad and/or the temperature assumption, but the detailed explanation is not known. It is supposed that σ_y and τ_{xy} also decrease with increasing thickness of pad because a thick Al pad similarly buffers σ_y and τ_{xy} .

Figure 8 shows the change in the maximum stresses in substrate with bonding time t over the range 1–100 ms. The experimental amplitude results were used in these calculations; the values of A_i and A_t (shown in Figure 3) were used as the inputs A_o and A_b in the simulation. However, as described above, A_i is slightly larger than A_t in the initial stages because of the measuring accuracy of A_i . Thus, A_b was assumed to be $0.99999 A_o$ in the initial stage ($t < 5$ ms). The thickness of the Al pad was set to $t_p = 4$ μm for calculating the results in Figure 8. As seen in Figure 8, the stress emerges in the substrate as t

increases from 0 to 5 ms, but it is not so large. From $t = 5$ to 10 ms, the maximum stresses sharply increase even though the interface seems to keep sliding (A_t is nearly equal to A_i) as shown in Figure 3. After 10 ms, maximum stresses gradually increase and saturate to a constant value. These results indicate that, at first, the ribbon slides on the substrate almost freely. As frictional adhesion emerges, strengthens, and the adhered areas expand, large shear stresses develop in the interface and stress in the substrate increases. Finally, the maximum stresses in the substrate remain steady because the developed adhesion areas strongly constrain the motion of the ribbon. σ_x reaches approximately 1 GPa after progression of ultrasonic bonding, and this large stress may damage the substrate during bonding.

Figure 9 shows experimental results for the interfacial shear stress up until $t = 100$ ms. The bonding condition was $F_b = 7.0$ N, $P_u = 2.5$ W. The shear stress applied at the interface between Al ribbon and SiO₂ substrate was measured with a piezoelectric load-cell. The trends in the experimental results resembles those of the calculation results, as shown in Figure 8, though the initial stage with free slip is very short in the experimental result. The interfacial shear stress is comparable to τ_{xy} in the calculations. τ_{xy} reaches approximately 300 MPa, and the interfacial shear stress reaches approximately 200 MPa. The stresses which occur in the substrate in the numerical simulation may be overestimated because all of ultrasonic vibration energy is assumed to be consumed around the bonding interface area. On the other hand, the experimental result is understood to be an underestimation because there is always energy loss in the measuring system. Although the stress evolution calculated in the present study may be overestimated, the numerical results are valid to some extent.

5. Conclusions

The amplitude of the interface and the stress evolution during ultrasonic Al ribbon bonding have been investigated and discussed. The following results were obtained:

- (1) The amplitude of the interface becomes smaller than that of tool-tip, and the difference between these amplitudes increases, with the progression of ultrasonic bonding.
- (2) Large stresses can occur in the substrate during ultrasonic bonding, and the stress increases with the progress of adhesion.
- (3) Thick Al pads can reduce the stress in the substrate during ultrasonic bonding.
- (4) The stress in the substrate increases with bonding time. The stress rapidly increases when adhered areas are formed at the interface. The stress stabilizes after adhered areas have developed.
- (5) Even if adhesion occurs during bonding, frictional slip can be produced.

Acknowledgments

The authors express their gratitude to Mr. Akira Hiram and nac Image Technology for their technical support and advice.

References

- [1] Ando M, Maeda M and Takahashi Y 2013 *Mater. Trans.* **54** 911
- [2] Takahashi Y, Suzuki S, Ohyama Y and Maeda M 2012 *J. Phys. Conf. Ser.* **379** 012028
- [3] Takahashi Y, Maeda M, Ando M, and Yamaguchi E 2015 *ibid.* in press
- [4] Maeda M, Yoneshima Y, Kitamura H, Yamane K and Takahashi Y 2013 *Mater. Trans.* **54** 916
- [5] Shah A, Rezvani A, Mayer M, Zhou Y, Persic J and Moon J.T 2011 *Microelectron. Reliab.* **51** 67
- [6] Seppänen H, Kurppa R, Meriläinen A and Hæggström E 2013 *Microelectron. Eng.* **104** 114
- [7] Mayer M, Schwizer J, Paul O, Bolliger D and Baltes H 1999 *Adv. Electron. Packag.* **26** 973
- [8] Maeda M, Yamane K, Matsusaka S and Takahashi Y 2009 *Quart. J. Jpn. Weld. Soc.* **29** 138
- [9] Gaul H, Shah A, Mayer M, Zhou Y, Schneider-Ramelow M and Reichl H 2010 *Microelectron. Eng.* **87** 537
- [10] Toshio H et al. 2012 *Chronological Scientific Tables 2012* (Tokyo: Maruzen) p 391
- [11] Oyama Y, Kitamura H, Maeda M and Takahashi Y 2009 *Proc. National Autumn Meeting of Jpn. Weld. Soc. (Tokushima)* **85** 449